ELSEVIER

Neurobiology of Disease

www.elsevier.com/locate/ynbdi
Neurobiology of Disease 31 (2008) 46 – 57

A transgenic rat that develops Alzheimer's disease-like amyloid pathology, deficits in synaptic plasticity and cognitive impairment

Li Liu, Ian J. Orozco, Emmanuel Planel, Yi Wen, Alexis Bretteville, Pavan Krishnamurthy, Lili Wang, Mathieu Herman, Helen Figueroa, W. Haung Yu, Ottavio Arancio, and Karen Duff*

Department of Pathology, Taub Institute for Research on Alzheimer's Disease, Columbia University, Black Building #5-513, 650 West 168th Street, New York, NY 10032, USA

Received 4 January 2008; revised 7 March 2008; accepted 15 March 2008
Available online 7 April 2008

In the last decade, multiple lines of transgenic APP overexpressing mice have been created that recapitulate certain aspects of Alzheimer's disease (AD). However, none of the previously reported transgenic APP overexpressing rat models developed AD-like β-amyloid (Aβ) deposits, or age-related learning and memory deficits. In the present study, we have characterized a transgenic rat model overexpressing transgenes with three, familial AD mutations (two in APP and one in PS1) that were developed by Flood et al. [Flood, D.G., et al., Aβ deposition in a transgenic rat model of Alzheimer's disease. Society for Neuroscience 2003, Washington, DC, 2003]. From the age of 9 months, these rats develop Aβ deposits in both diffuse and compact forms, with the latter being closely associated with activated microglia and reactive astrocytes. Impaired long-term potentiation (LTP) was revealed by electrophysiological recordings performed on hippocampal slices from rats at 7 months of age, which is 2 months before the appearance of amyloid plaques. The deficit in LTP was accompanied by impaired spatial learning and memory in the Morris water maze, which became more pronounced in transgenic rats of 13 months of age. For Tg rats of both ages, there was a trend for cognitive impairment to correlate with total Aβ42 levels in the hippocampus. The rat model therefore recapitulates AD-like amyloid pathology and cognitive impairment. The advantage of the rat model over the available mouse models is that rats provide better opportunities for advanced studies, such as serial CSF sampling, electrophysiology, neuroimaging, cell-based transplant manipulations, and complex behavioral testing.

Keywords: Alzheimer's disease; Transgenic rat; β-Amyloid peptide; Amyloid plaques; Synaptic plasticity; Long-term potentiation; Learning and memory

Introduction

Alzheimer's disease is characterized by the progressive loss of cognitive abilities associated with increased brain β-amyloid (Aβ) levels, extracellular Aβ deposited in senile plaques, intraneuronal neurofibrillary tangles, loss of synapses, and neuronal cell death (Selkoe, 2001). Autosomal dominant mutations in three genes — amyloid precursor protein (APP) on chromosome 21, presenilin-1 (PS1) on chromosome 14 and presenilin-2 (PS2) on chromosome 1 (reviewed in Selkoe, 2001) cause an early onset form of AD, that is clinically and pathologically indistinguishable from late onset, sporadic AD. A common property of these mutations is that they increase the production of Aβ, especially the 1–42 amino acid form (Aβ42), which enhances Aβ aggregation in the brain. These findings form the theoretical basis of the amyloid hypothesis that proposes that increased Aβ (but not necessarily as plaque β-amyloid) plays a central role in the pathogenesis of AD (Hardy and Selkoe, 2002). Indeed, mounting recent evidence suggests that a diffusible, oligomeric form of the Aβ is causative of synaptic dysfunction, which underlies the earliest AD syndrome prior to neuronal degeneration (Selkoe, 2002).

In the last decade, multiple lines of transgenic (Tg) mice overexpressing one or more of these familial AD linked genes have been created (McGowan et al., 2006). Although none of the mouse models recapitulate all aspects of AD, several lines do develop robust AD-like pathology, including Aβ containing plaques surrounded by phospho-tau containing dystrophic neurites, synaptic damage, and age-related learning and memory deficits (McGowan et al., 2006). These transgenic mouse models have provided new opportunities to investigate the biochemical and cellular mechanisms underlying this devastating neurodegenerative disorder, and have helped identify the link between elevated Aβ and synaptic dysfunction. Long-term potentiation (LTP) is an indicator of synaptic plasticity, which underlies learning and memory. Impaired LTP has been demonstrated in several transgenic AD mouse models (Chapman et al., 1999; Trinchese et al., 2004; Oddo et al., 2003; Gureviciene et al.,

* Corresponding author.
E-mail address: ked2115@columbia.edu (K. Duff).
Available online on ScienceDirect (www.sciencedirect.com).

0969-9961/$ - see front matter © 2008 Elsevier Inc. All rights reserved.
doi:10.1016/j.nbd.2008.03.005

2004). In parallel with the generation of transgenic mice, several transgenic rat models have also been produced as rats are a better rodent model for studies involving neurobehavioral testing, cannulation, sampling of cerebrospinal fluid, electrophysiology, neuroimaging and cell-based transplant manipulations (Abbott, 2004). The first Tg rat line was generated by Flood et al. at Cephalon, Inc and is described in an abstract (Flood et al., 2003). These rats have mutations in APP (K670N/M671L and V717F) and PS1 (M146V), and they have been reported to develop amyloid deposits around the age of 9 months; however, further studies, such as cognitive performance, electrophysiology etc, have not been demonstrated. A second rat model was reported in 2004 (Ruiz-Opazo et al., 2004) that expresses human APP harboring the K670N/M671L (Swedish) mutations. This rat expressed low levels of human APP, and amyloid pathology was not observed. However, these transgenic rats performed better than age-matched controls in the Morris water maze tasks. In the same year, Echeverria et al. reported a third rat model that accumulated intracellular Aβ in the hippocampus and cerebral cortex, but failed to develop extracellular amyloid deposits (Echeverria et al., 2004). Very recently, a fourth transgenic rat expressing Swedish mutant human APP has been reported to develop mild, extracellular Aβ immunostaining, but this rat also failed to develop compact, mature amyloid plaques by the age of 22 months (Folkesson et al., 2007). Thus, to date, no published transgenic APP rat line develops robust amyloid neuropathology, or cognitive deficits. In the present study, we have characterized the transgenic rat model developed by Flood et al. (2003) and have demonstrated that by 9 months of age, robust amyloid plaques primarily composed of Aβ42 develop in the brain, mainly in the hippocampus. A proportion of these plaques are associated with activated microglia and reactive astrocytes. Prior to plaque appearance, the transgenic rats at 7 months of age showed a deficit in LTP compared to age and gender matched non-transgenic, wild type rats. A deficit in spatial learning and memory was seen in the transgenic rats at this and also later age, when plaques have formed, and the degree of impairment showed a strong trend to correlate with the level of total Aβ42 in the hippocampus.

Materials and methods

Animals

Transgenic rats used in the present study were homozygous for mutant APP and PS1 (Flood et al., 2003) and were on the inbred Sprague–Dawley background. Line 478 expressing the Ceph 12 construct (rat synapsin I promoter and human APP 695 with the familial AD K670N/M671L mutations) were crossed with line 1116 rats expressing the sisAPP69-NLF construct (PDGFβ promoter and human APP695 with the familial AD K670N/M671L and V717F mutations) and the offspring were inbred to generate rats homozygous at both loci. Double Tg rats were crossed to the third transgenic line, line 11587 expressing the 1015 construct (rat synapsin I promoter and human PS1 with the familial AD M146V mutation). The Tg rats used in our study were obtained by in-breeding homozygous rats expressing the three transgenes. Age-matched, male Sprague–Dawley rats were purchased at 6 months of age from Harlan Inc then housed under identical conditions to the transgenics and used at the same age. The Tg and wild type rats were both Sprague–Dawley background. Throughout the study-period, the animals were housed individually in a controlled environment (temperature 22 °C, humidity 50–60%, light schedule from 0700 to 1900). Animals were used in full compliance with the National Institutes of Health/Institutional Animal Care and Use Committee guidelines.

Antibodies

Three mouse monoclonal anti-Aβ antibodies were used: 6E10 (recognizes aa 1–10, Signet), JRF/cAβ40/10 (aa 35–40) and JRF/cAβ42/26 (aa 36–42) (Centocor) (Refolo et al., 2001). GFAP polyclonal antibody, and synaptophysin and PSD95 monoclonal antibodies were purchased from Sigma, mouse anti-rat CD11b antibody was purchased from Serotec Inc. Monoclonal APP antibody, 22C11, was purchased from Chemicon. The Ab14 antibody against N-terminal fragment of PS1 was provided by Dr. Sam Gandy (Mt Sinai Medical Center, NY). Tau A0024 (DakoCytomation) was used to detect total tau. The phospho-tau antibodies AT8 (S202/205) and AT270 (T181) were from Pierce; CP13 (S202) and PHF-1 (S396/404) were the generous gift of Dr. Peter Davies (Albert Einstein Medical Center, NY).

Slice preparation and LTP recording

Seven month-old Tg and age-matched wild type rats were decapitated and their hippocampi were removed. Transverse hippocampal slices (400 μm) were maintained in an interface chamber at 29 °C as described previously (Vitolo et al., 2002). They were perfused with saline solution (124.0 mM NaCl, 4.4 mM KCl, 1.0 mM Na_2HPO_4, 25.0 mM $NaHCO_3$, 2.0 mM $CaCL_2$, 2.0 mM $MgSO_4$, and 10 mM glucose) continuously bubbled with 95% O_2 and 5% CO_2. Slices were permitted to recover from cutting for at least 90 min before recordings. The fEPSPs were recorded from the CA1 region of the hippocampus by placement of both the stimulating and the recording electrodes in the CA1 stratum radiatum, as described previously (Vitolo et al., 2002). BST was assayed by plotting the stimulus voltage intensity (V) against the slopes of the fEPSP to generate input–output relations or by plotting the peak amplitude of the fiber volley against the slope of the fEPSP to generate input–output relations. LTP was induced using theta-burst stimulation (4 pulses at 100 Hz, with the bursts repeated at 5 Hz, and each tetanus including 3, 10-burst trains separated by 15 s). Each point of the graphs represents the average of 5 successive events. The data are reported as the mean±SEM.

Histopathology

The PSAPP transgenic rats were transcardially perfused with ice-cold PBS under deep anesthesia, and the brains were rapidly removed after decapitation. One hemibrain was immersed in 4% paraformaldehyde in PBS for 48 h, and then transferred to a 30% sucrose solution, in which it was kept overnight on a shaker table for cryoprotection. The other hemibrain was dissected on ice into selected brain areas (hippocampus and cortex) that were stored in −80 °C for biochemical assays. Brain sections (40 μm) were cut using a cryostat. Free-floating brain sections were applied for immunohistochemistry using SuperPicTure™ polymer detection kit and a Picture Plus double staining kit (for Aβ and GFAP double staining) (Zymed, San Francisco, CA). Sections were washed with PBS for 10 min, and then treated with 3% H_2O_2 in PBS for 10 min. For certain antibodies, epitope retrieval was also performed using sodium citrate buffer (10 mM sodium citrate, 0.05% Tween 20, pH

6.0). The sections were then transferred to a microfuge tube that contained 1 ml of primary antibody diluted in PBS containing 0.3% Triton and 5% normal serum, and incubated at RT for 1 hour on a rotator. After three washes with PBS-T (0.1% Triton-X 100), the sections were incubated for 10 min with HRP polymer conjugate. Following three washes with PBS-T (0.1% Triton-X 100), the immunoreactive material was visualized using DAB as chromogen. The stained sections were mounted on slides and inspected by light microscopy. Brains from age-matched wild type (Wt) controls, or PSAPP mice, (Holcomb et al., 1998) were used as either negative or positive controls, respectively. Silver staining of brain sections was performed using the FD NeuroSilver™ Kit II (FD Neurotechnologies Inc., MD) following manufacturer's instruction. Thioflavin-S (0.2% in ddH2O) staining was performed in brain sections alone or following the silver staining as a counterstain (Wengenack et al., 2000). Brain sections from a 9 month-old PSAPP mouse were stained together with Tg rat brains for comparison.

Immunoblotting

Frozen hemispheres were weighed and homogenized without thawing in 5× volume/weight of modified RIPA buffer [50 mM Tris–HCl, pH 7.4, 1% NP-40, 0.25% Na-deoxycholate, 150 mM NaCl, 1 mM EDTA, 1 mM PMSF, 1 mM Na_3VO_4, 1 mM NaF, 10 µl/ml protease inhibitor mixture P8340 (Sigma)], with a mechanical homogenizer (TH; Omni International, Marietta, GA). Samples were then centrifuged for 20 min at 20,000 ×*g* at 4 °C, and protein content of the supernatants was determined. The supernatants were diluted 1/10 in O+ buffer [62.5 mM Tris–HCl, pH 6.8, 10% (w/v) glycerol, 5% 2-mercaptoethanol, 2.3% SDS, 1 mM EGTA, 1 mM EDTA, 1 mM PMSF, 1 mM Na_3VO_4, 1 mM NaF, 10 µl/ml protease inhibitor mixture P8340 (Sigma)] and boiled for 5 min (37 °C for presenilin 1). Depending on the antibody used, 7–21 µg of protein were analyzed as described previously (Planel et al., 2007).

Aβ ELISA

Levels of human Aβ40 and Aβ42 in brain extracts and plasma were quantified by ELISA using antibodies supplied by Centocor (Refolo et al., 2001), as described previously (Schmidt et al., 2005a; Schmidt et al., 2005b). Hemibrains were homogenized in 20 mM Tris buffer containing 1 mM EDTA, 1 mM EGTA, 250 mM sucrose, and protease inhibitors, pH 7.4. A two-step extraction was then performed. In the first step soluble Aβ was extracted using diethyl acetate (DEA) 0.4% in 100 mM NaCl and the sample was centrifuged at 135,000 ×*g* for 60 min. The supernatant was neutralized by adding 0.5 M Tris–HCl, pH 6.8. In the second step, insoluble plaque associated Aβ was extracted by the addition of 70% formic acid (FA). The ELISA assay was performed as described previously (Refolo et al., 2001). Briefly, Nunc-immuno plates (Maxisorp; Nunc A/S, Roskilde, Denmark) were coated with 10 µg/ml JRF/cAβ40/10 or JRF/cAβ42/26 (Refolo et al., 2001). Freshly thawed samples were diluted and incubated overnight. Signal was detected using a horseradish peroxide-labeled antibody, JRF/AbN/25, which is human Aβ specific. Assays were developed with TMB/H_2O_2 substrate (Pierce, Rockford, IL, USA) according to the manufacturer's specifications.

Morris water maze

Transgenic and wild type rats of 7 months or 13 months of age were used in this study. Twelve Tg rats (6 male and 6 female) and 8 Wt (4 male and 4 female) rats were tested at the age of 7 months; nine Tg (male) and 8 Wt (male) rats were tested at the age of 13 months in the Morris water maze (MWM). The water maze apparatus consisted of a circular aluminum pool, 170 cm in diameter (Stoelting Co.) and a movable round platform (10 cm × 10 cm, transparent). The pool was filled with water (22 ± 1 °C) and rendered opaque by the addition of non-toxic white paint. The top surface of the platform was 2.0 cm below the water line. The pool was divided into 4 imaginary quadrants (north, south, east and west), and a video-computer tracking system (HVS Image®, Hampton, UK) was used to record the rats' swim path for later analysis (Water 2020® software, Hampton, UK). Large posters on the wall of the room served as visual cues. Before the start of training, animals were habituated to the pool without a platform for 1 min/day, for 3 days.

The rats were first trained to find the hidden platform that was kept in the middle of one of the four quadrants throughout the five days of testing (spatial version of the MWM task). A trial was initiated by placing the rat in the water facing the pool wall in one of the other three quadrants (which did not contain the platform) in a semi-random order that varied each day. They were tested for four trials per day, with an inter-trial interval of 3–5 min, beginning from other three different start points. If a rat failed to find the hidden platform within 60 s (or 90 s for the 13 month-old rats), the experimenter gently placed it there for 15 s. The escape latency (time to reach the platform) and the length of the path that the animal swam to find the platform were used to assess acquisition of the water maze task. Swim speed (path length/escape latency) was used to assess the motor activity of rats. Twenty-four hours after the completion of training, the platform was removed and the rat was released into the quadrant diagonally opposite to that which previously contained the platform. During this probe trial, the rat was allowed to search for 60 s (or 90 s for the 13 month-old rats), without the platform. This test was used to assess how well the rats remember the location of the platform (i.e. retention of memory).

To test the visual acuity of the rats and their motivation to escape, a cued version of WM task was conducted following the hidden platform training with all visual cues on the wall removed. The rats were given four trials, and were trained to find a cued-platform that had a 10-cm-high black–white pole. The platform was changed to a novel position semi-randomly from trial to trial, and the rats were released into the water from positions that were opposite to the platform. Rats were tested counterbalanced with respect to subject groups.

Open field

The test was an automated version of the classic open-field test used to assess exploratory activity and anxiety in rats (Kauppila et al., 1991; Kumlin et al., 2007; Meerlo et al., 1996). The rat was placed at the center of a white-walled, circular arena (diameter 120 cm) and was allowed to move freely for 5 min. The movement path was recorded by video camera connected to a video tracker (HVS Image®, Hampton, UK), and the information was stored digitally on a PC. The distance traveled, running speed and the time spent in the middle relative to the periphery were recorded automatically, and analyzed later using the Water 2020® software (Hampton, UK).

Elevated plus-maze

This test has been described previously (Kauppila et al., 1991; Pellow et al., 1985). The maze was painted black and consisted

of two closed arms (50×10 cm, height 30 cm) and two open arms (50×10 cm) standing 50 cm above the floor (San Diego Instrument, CA). The rat was placed on the center platform facing an open arm and was allowed to explore the maze for 5 min. The number of entries into the open and closed arms, and the time spent on the open and closed arms were recorded semi-manually with a custom-made computer program (Kumlin et al., 2007). Relative time spent in the open arms was taken as a measure of anxiety.

Statistical analysis

Statistical analyses were carried out using SPSS for Windows (version 13.0, SPSS Inc., USA) or Prism 4 software. The effects of rat genotype, training day/trial, and their impact on water maze performance were analyzed by univariate analysis of variance (ANOVA) for repeated measures. The effect of genotype on the magnitude of the fEPSP was analyzed by two-way ANOVA (Prism 4 Software). The genotype effects on performance in open-field and elevated plus-maze were analyzed by independent Student *t*-tests. The data are reported as the mean±SEM. The correlation between hippocampal Aβ42 level, and water maze learning was analyzed using Pearson's r.

Results

Histopathology

Histopathology assessment of the PSAPP Tg rats was performed at the age of 4 months ($n=3$), 7 months ($n=3$), 13 months ($n=6$), and 19–22 months ($n=4$). No Aβ deposits were detected in the brain of Tg rats at 4–7 months of age with the antibodies used (6E10 or Aβx-40 and Aβx-42 specific antibodies). Aβ immunoreactive deposits were readily detected in the brains of rats at 13 or 19–22 months of age. The affected areas include cerebral cortex, hippocampal formation, olfactory bulbs, thalamus and hypothalamus, whereas cerebellum and brain-stem were free of Aβ deposits. Compared to other areas, the hippocampal formation had the highest Aβ load (for both 6E10 and JRF/cAβ42/26 antibody), which increased about 5 fold from 13 months (~5%) to 19–22 months of age (~25%). Most of the amyloid was in the form of diffuse plaques that were positively immunoreactive to anti-Aβ antibodies, but negative for silver staining or Thioflavin-S staining. However, a small number of amyloid plaques did stain positively for both silver and Thioflavin-S (Figs. 1D, F, G H); these plaques were defined as compact plaques that contain mainly fibillar amyloid in the β-sheet pleated conformation [note the consistency between silver (Fig. 1G) and Thioflavin-S staining (Fig. 1H) for the compact plaques]. Argyrophilic plaques were morphologically similar to those of the PSAPP transgenic mice (Holcomb et al., 1998), but less dense even at the age of 22 months. In general, the distribution pattern of immunostaining with 6E10 Aβ-antibody (Fig. 1A) was similar to that obtained with JRF/cAβ42/26 that is specific for Aβ42 (Fig. 1B). These antibodies labeled both diffuse and silver-stained Aβ deposits. In contrast, JRF/cAβ40/10, an Aβ40 specific antibody, labeled mainly the silver-stained/Thioflavin-S positive plaques (Fig. 1C). In Tg rats aged 19–22 months, we occasionally saw very weak anti-Aβ40 positive staining on the blood vessels of pia matter that was less typical than in the Tg mouse models (e.g. Winkler et al., 2001); however, no vascular Aβ deposits were detected in the parenchyma up to 22 months of age by any Aβ antibodies used in our study. The distribution of Aβ40 immunostaining paralleled that of the silver staining (Figs. 1C/E vs. D/F). Amyloid deposits were rarely

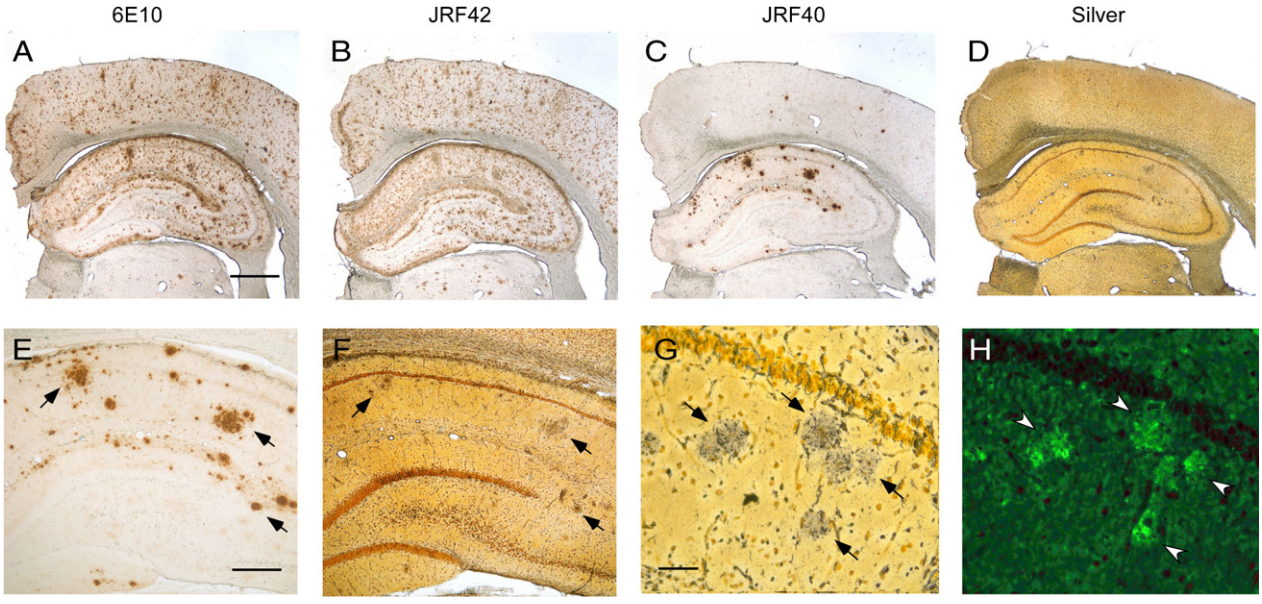

Fig. 1. Deposition of Aβ variants in the brain of a 19 month-old PSAPP transgenic rat. A–D. Four photomicrographs demonstrating adjacent coronal sections of the dorsal hippocampus. A–C. Brain sections were immunostained for Aβ, with 6E10 (Aβ1-x/Aβ total), JRF/cAβ42/26 (aa 36–42), and JRF/cAβ40/10 (aa 35–40), respectively; D shows an adjacent section to C that was stained with silver. E and F are higher magnifications of C, and D. Photomicrographs G and H demonstrate that the fibrillar Aβ deposits can be detected by both silver stain and Thioflavin-S. (G) shows the silver-stained plaques in the hippocampus, and the same plaques were identified by counterstaining with Thioflavin-S (H). The arrows point to amyloid plaques in E, F, G, and H. Scale bar is equal to 1000 μm for A, B, C, D, 250 μm for E, F, and 100 μm for G and H.

detected in the stratum pyramidale of the CA areas, and the granule cell layer of the dentate gyrus, whereas the deposits were present throughout other areas of the hippocampal formation. The density of Aβ deposits was highest in the outer part of the molecular layer of the dentate gyrus, followed by the subiculum, and other laminae. In the cortical areas, frontal cortex contained the highest density of amyloid deposits, followed by the parietal cortex. Although diffuse amyloid deposits can be readily detected, the number of compact plaques was very limited, and they mainly appeared in the hippocampus (see Figs. 1F, 3A, and E). A small number of diffuse Aβ deposits were observed in subcortical areas, such as striatum, septum, thalamus, and hypothalamus (not shown). Due to limited number of female Tg rats available for histopathology, we were unable to conclude whether or not there is a difference in pathology between the two genders.

Astrocyte reactivity to the amyloid deposits was evaluated with GFAP immunostaining. In the wild type animals, GFAP immunostaining of quiescent astrocytes was largely restricted to the hippocampus (Fig. 2A) and white matter tracts such as the corpus callosum. In the 13–22 month-old transgenic rats, the overall intensity of GFAP immunoreactivity was increased considerably (Fig. 2B), and clusters of reactive astrocytes stained with GFAP were visible surrounding the amyloid plaques, as demonstrated by Aβ and GFAP double-labeling (Fig. 2C). The reactive astrocytes were ramified, and the processes were thickened and darkly stained (Fig. 2C). In the Tg rat brain, there were a small number of activated microglia, and they were strongly immunoreactive to anti-CD11b antibodies, and in close association with the silver-stained amyloid plaques (Figs. 2D–F).

In addition, Tg rat brain sections were also stained with antibodies recognizing phospho-tau, including antibody AT8, which recognizes tau phosphorylated at Ser202/Thr205, CP13 (Ser202), and PHF-1 (Ser396/404) (Andorfer et al., 2003). Neurofibrillary pathology in the form of neuropil threads, abnormal somato-dendritic accumulation of tau or tangles was not observed in 19–22 month-old rats, but these antibodies did reveal phospho-tau containing speckles in the hippocampus, which were closely associated with the compact plaques (Fig. 3). The morphology of the immunoreactive material was similar to the dystrophic neurites that were described previously in the PSAPP Tg mice (Kurt et al., 2003). Stained serial sections demonstrated that AT8 immunoreactive punctae co-localized with silver-stained plaques (Figs. 3A–D). Dystrophic neurites labeled by PHF-1 and CP13 were detected in the hippocampus, and they were also associated with the large, compact amyloid plaques (Figs. 3E–H). No changes were detected by immunoblotting analysis in total tau (Tau-C positive) or phospho-tau (PHF-1, CP13, AT270 positive) protein levels in brain lysates from 7 month-old Tg rats compared to Wt rats (data not shown). Cresyl violet staining was performed to visualize cell bodies. Overall, the cytoarchitectural organization of the cerebral cortex and hippocampus appeared normal, and overt cell loss was not detected in the brains of 13- and 19–22 month-old Tg rats. Gross synaptic integrity was examined by immunohistochemistry using an antibody against synaptophysin. No obvious difference in the intensity or pattern of synaptophysin immunoreactivity was found in 22 month-old rats compared to controls. In line with this data, we were unable to detect any difference in protein levels of synaptophysin and PSD-95, two representative synaptic markers, in the brain lysate from Tg rats compared to Wt rats at either 7 months or 13 months of age (data not shown).

Electrophysiology

Hippocampal slices from 7 month-old male Tg animals were assessed for defects in synaptic physiology at the Schaffer collateral-

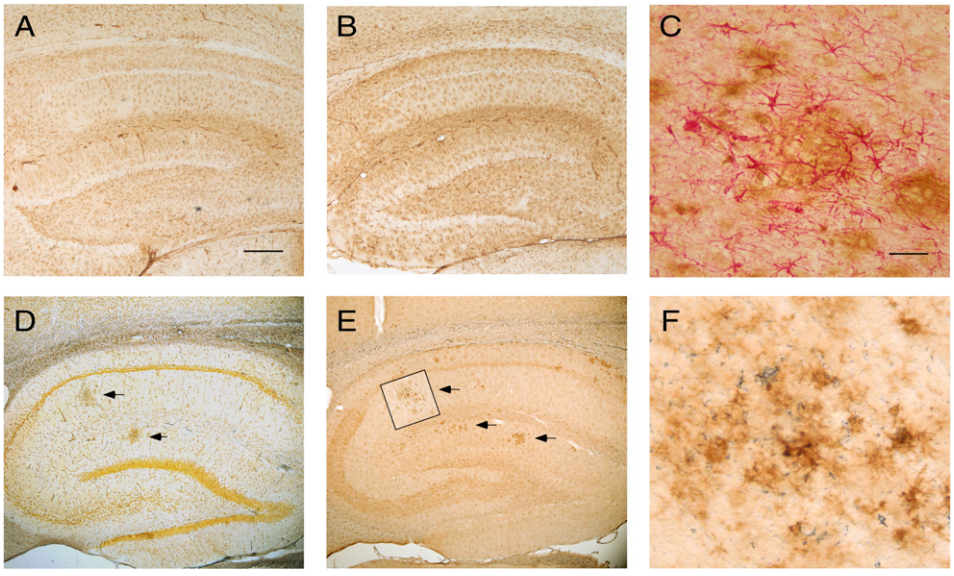

Fig. 2. Immunostaining of astrocytes and microglia in 19–22 month-old PSAPP Tg rats. A, B, Sections were immunostained for GFAP antigen from age-matched Wt (A), and 19 month-old Tg rat (B). Quiescent astrocytes were stained with GFAP antibody in the Wt rat (A); however, Tg rat showed increased GFAP immunoreactivity in general, in addition to focally enhanced staining of reactive astrocytes. C, Double labeling of Aβ and GFAP demonstrates the close association of reactive astrocytes with amyloid plaques. The GFAP positive astrocytes are in red, and the amyloid plaques are in brown. D, E, Adjacent sections silver-stained for amyloid (C) and immunostained for CD11b antigen (D), demonstrate the close association of activated microglial cells and compact amyloid plaques. The arrows point to amyloid plaques in D, and activated microglial cells in E. Details of the boxed area in E is shown with higher magnification in F. Scale bar is equal to 500μm for A, B, D, E, and 50 μm for C and F.

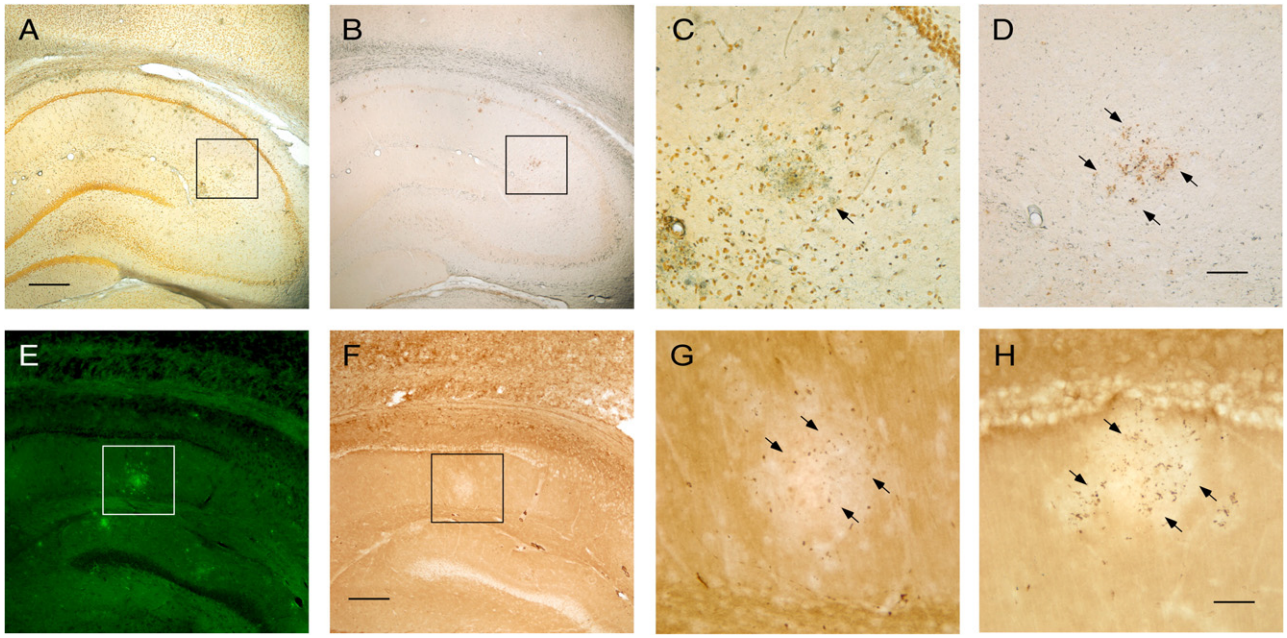

Fig. 3. Dystrophic neurites surrounding fibrillar amyloid deposits stained with antibodies specific for phospho-tau in 19–22 month-old Tg rats. A, B, Two photomicrographs demonstrating silver-stained amyloid plaques (A) and associated AT-8 immunostaining (B) from adjacent sagittal sections of the hippocampus. Higher magnification of the boxed area in A and B are shown in C and D. Similarly, photomicrographs E, F demonstrate, on adjacent sections, that the PHF-1 immunoreactive neurites (see G, the boxed area in F) are in close association with the compact Aβ plaques stained with Thioflavin-S (E). CP13 antibody revealed similar dystrophic neurites around the compact Aβ plaques (H). The arrows point to amyloid plaques (C), and phospho-tau immunoreactive staining (D, G, H). Scale bar is equal to 500 μm for A, B, 100 μm for C, D, 400 μm for E, F, and 50 μm for G, H.

CA1 connection. To test for altered basal synaptic transmission, input–output curves were generated by plotting the field excitatory post-synaptic potentials (fEPSPs) at CA1 as a function of increasing stimulation intensities delivered to the Schaffer collaterals pathway (Fig. 4A). No statistical difference in the magnitude of the fEPSPs evoked with stimulation intensities ranging between 5 and 35 V were found by two-way ANOVA ($F[1,20]=0.08$, $P>0.05$). At the maximal stimulation intensity of 35 V, Tg animals generated, on average, fEPSPs of similar magnitude compared to age-matched male Wt control animals (1.8±0.2 V/s, 12 slices from five Tg animals versus 1.8±0.2 V/s, 10 slices from six control animals).

LTP is widely believed to be a molecular correlate of learning and memory and it is monitored to evaluate deficits in synaptic plasticity. Following a stable 10-minute baseline of fEPSPs of similar magnitude, a theta-burst stimulation was given to the Schaffer collateral pathway. High frequency stimulation results in an enhanced fEPSP response lasting hours. In slices from Tg animals, the magnitude of the fEPSP (relative to the baseline), 1 h after the stimulation, was largely reduced in comparison to slices from age-matched, control animals (153%±9%, 12 slices from 5 Tg animals versus 199%±13%, 10 slices from 6 control animals) (Fig. 4B). Statistical analysis by two-way ANOVA showed a significant effect by genotype ($F[1,20]=9.68$, $P<0.01$).

Behavioral studies

The Morris water maze test was performed to examine hippocampal-dependent spatial learning and memory. Transgenic and wild type rats at 7 months or 13 months of age showed no motor deficits as they were able to climb onto the platform and showed no deficits in swimming ability during the training. Twelve Tg rats and 8 Wt rats were tested at the age of 7 months, prior to the formation of amyloid plaques but at an age when the Tg rats showed a deficit in LTP. In the spatial version of the water maze test, the swim speed did not differ between Tg and Wt rats [$F(1,18)=1.02$, $P>0.30$]. During the five days of training, both Tg and Wt rats significantly improved their performance as shown by reduced escape latency to reaching the platform (and also shortened distance) [$F(1,18)=78.98$, $P<0.001$] (Fig. 5A); however, the average latency that Tg rats needed to find the hidden platform was significantly longer [$F(1,18)=8.66$, $P<0.01$] than that of the control rats, indicating that the PSAPP rats had a spatial learning and memory deficit (Fig. 5A). During the probe trials in which the rats tried to find the hidden platform, the percentage of time Wt rats spent in the target area was significantly higher than the time spent in any of the other three quadrants [one-sample t-test, $t(7)=3.59$, $P<0.01$, test value=25]. In contrast, Tg rats spent ~30% of the time in the target quadrant which was not significantly different from the 25% chance level [one-sample t-test, $t(11)=1.97$, $P>0.75$, test value=25] (Fig. 5B).In the non-spatial version of the water maze test, Tg and Wt rats performed equally well in locating a cued-platform [escape latency, $F(1,17)=0.01$, $P=0.98$], which indicated that the Tg and Wt rats had comparable motor ability and visual acuity. The lack of preference for the target quadrant, together with overall poor performance during training suggested that the Tg rats had impaired spatial learning and memory before the appearance of amyloid plaques (Fig. 5B). We also compared the water maze performance of the male and female Tg rats ($n=6$ for each sex) but no statistical difference was found for escape latency [$F(1,10)=0.29$, $P=0.60$] (or swim distance) implying that both sexes were impaired in spatial learning and memory.

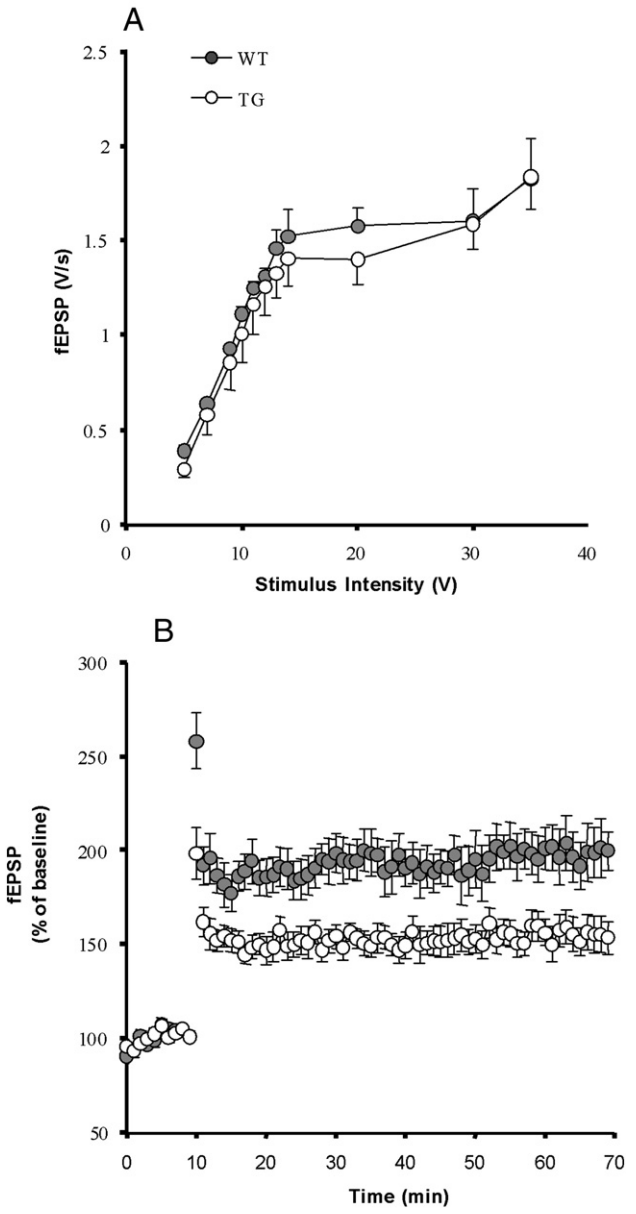

Fig. 4. Seven month-old PSAPP rats demonstrated normal basal synaptic transmission (BST) in the cornu ammonis 1 (CA1) region of the hippocampus, but reduced long-term potentiation (LTP), a measure of synaptic plasticity. (A) Input–output plots showing the relationship between field excitatory post-synaptic potential (fEPSP) slopes and stimulus intensity recorded from the CA1 region of slices prepared from 6–8 month-old wild type (Wt) (filled circles) ($n=10$ slices from 6 animals) and PSAPP rats (open circles) (12 slices from 5 animals). (B). Plots showing the amount of potentiation following theta-burst stimulation in the CA1 region of slices prepared from 7 month-old wild type (Wt) (filled circles) ($n=10$ slices from six animals) and PSAPP rats (open circles) (12 slices from five animals).

The second group of rats (all male, Tg, $n=9$, Wt, $n=8$) were tested in the water maze at the age of 13 months, when amyloid plaques had already formed. In the non-spatial, cued-platform version of the water maze, no group difference in swim speed [$F(1,15)=1.60$, $P=0.23$] or escape latency was found between the Tg and Wt rat groups [escape latency, $F(1,15)=2.31$, $P=0.13$]. Both Tg and Wt rats significantly improved their performance during the hidden platform training as shown by reduced escape latency and shortened distance swam to locate the platform [for latency, $F(1,15)=109.0$, $P<0.001$] (Fig. 5C). However, similar to the 7 month-old group, the performance of the 13 month-old Tg rats was significantly inferior to that of the Wt rats, i.e. the time and swim distance that Tg rats needed to locate the hidden platform were significantly longer than those of the Wt rats [for latency, $F(1,15)=17.45$, $P=0.001$] (Fig. 5C). During the probe trial, Wt rats showed a exclusive preference for the target zone containing the platform [one-sample t-test, $t(7)=7.78$, $P<0.001$, test value=25], whereas Tg rats spent only chance level (~26%) of the time in the target quadrant [one-sample t-test, $t(8)=0.602$, $P=0.56$, test value=25] (Fig 5D). Together these findings suggested that the older Tg (13 month-old) rats also had impaired spatial learning and memory, which was more pronounced than in the younger Tg rats (7 month-old).

As differences in locomotor/exploratory activity or status of anxiety/fear could affect water maze performance (e.g., Schulz et al., 2007; Herrero et al., 2006), we further tested the Tg and Wt rats at 7 and 13 months of age in the open-field (locomotor and exploratory activity) and the elevated plus-maze (anxiety-like behavior). In the open-field test, no difference was found in the total distance traveled (7 month-old, [$t(1,18)=-1.07$, $P=0.29$]; 13 month-old, [$t(1,13)=0.98$, $P=0.34$]) and the running speed (7 month-old, [$t(1,18)=-1.07$, $P=0.30$]; 13 month-old, [$t(1,13)=0.99$, $P=0.34$]) between the Tg and the Wt rats (for 13 month-old, see Fig. 5E). For both ages, the time spent by the Tg rats in the outer zone and in the center zone was not statistically different from that of the Wt rats (7 month-old, outer zone [$t(1,24)=-0.897$, $P=0.39$], center zone [$t(1,24)=-0.89$, $P=0.38$];13 month-old, outer zone [$t(1,13)=1.28$, $P=0.23$], center zone [$t(1,13)=-1.28$, $P=0.23$]). In the elevated plus-maze test, both ages of Tg and Wt rats spent most of the time in the closed arms during the 5-minute test time (for 13 month-old, see Fig. 5F). No group difference was observed in the percentage of time spent in the open arm (7 month-old, [$t(1,24)=-0.60$, $P=0.55$]; 13 month-old, [$t(1,12)=0.60$, $P=0.56$]).

APP, PS1 and brain Aβ levels: relation to cognitive deficits

The brain levels of APP and PS1 protein in the PSAPP Tg rats were compared to wild type rats by quantitative immunoblotting using the 22C11, and the Ab14 antibodies, respectively. PSAPP Tg rats had ~2 fold increase in both APP (Fig. 6, upper panel) and PS1 levels compared to Wt rats (Fig. 6, lower panel). Brain Aβ peptide levels were measured by ELISA using human Aβ42 and Aβ40 specific antibodies. Hippocampus and cerebral cortex were analyzed separately because Aβ plaques developed at different rate in these areas. Between ~7 and ~13 months of age, total Aβ levels increased greatly, about 15 fold (for either Aβ40 or 42) in the hippocampus, and 5 fold (Aβ40) or 50 fold (Aβ42) in the cortex. The level of Aβ42 in the hippocampus was 3 times higher than in cortex; for Aβ40 it was 16 fold higher (Table 1, the values shown are mean±SEM). This was consistent with the higher plaque burden in hippocampus revealed by immunohistochemistry. The Aβ42:Aβ40 ratio increased greatly for both hippocampus and cortex, with the cortex having a higher degree because it had a lower basal Aβ level compared to the hippocampus. No amyloid plaques were seen in 7 month-old rats. In the 13 month-old rats, the Aβ load measured by immunohistochemistry with Aβ-antibody (6E10/JRFAβ42) (Liu et al., 2002) was consistent with the Aβ levels measured by ELISA (data not shown). The percentage of time spent in the target quadrant during the probe trial has been

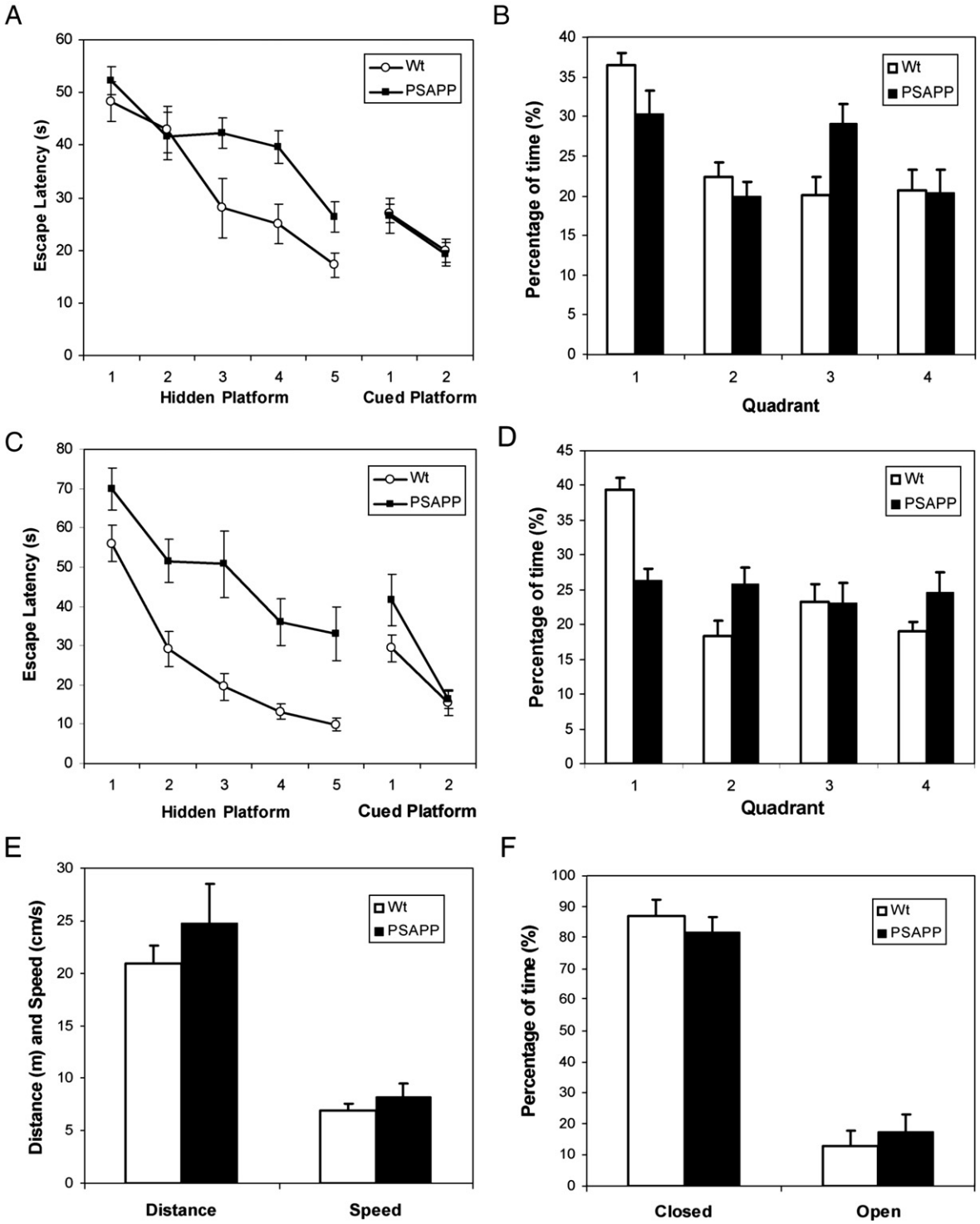

Fig. 5. PSAPP Tg rats were impaired in spatial learning and memory in the Morris water maze, while they did not differ from Wt rats in locomotor activity and level of anxiety. The results of water maze tests were shown in A, B (for 7 month-old rats) and C, and D (for the 13 month-old). A and C, Escape latency to the hidden platform. The group averages for the four daily trials ± SEM are given. B and D, Search bias during the probe trial 24h after the last training trial of day 5. Wt rats spent significant amount of time in the target area (quadrant 1), whereas Tg rats did not show a spatial bias to this quadrant. The columns indicate the percentage of time (mean + SEM) spent in the previous platform quadrant (quadrant 1) and three other quadrants (quadrant 2–4). E, Behavioral parameters of the open-field tests. The numbers on the y axis indicate distance traveled (m), and running speed in cm/s, respectively. Group means + SEM are given. No significant difference was found between the Tg and Wt rats. F, Percentage of time spent in the closed and open arms during the 5-min plus-maze test. Group means + SEM are given. No significant difference was found between the Tg and Wt rats.

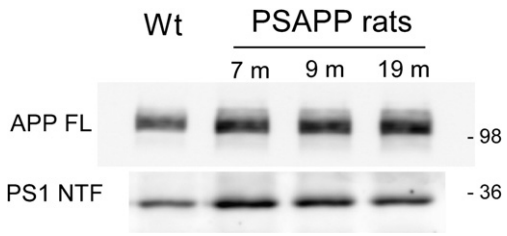

Fig. 6. The level of APP protein in the PSAPP Tg rats (7, 9, and 19 months) was compared to Wt rats (9 months) using the 22C11 monoclonal antibody. PSAPP Tg rats had ~2 fold more APP than Wt rats (upper panel). The level of PS1 derived N-terminal fragment in the Tg as detected by the Ab14 antibody showed also ~2 fold increase compared to Wt rats (lower panel).

most widely used as a score for hippocampal-dependent learning and memory (learning-memory score) (Liu et al., 2003; Santacruz et al., 2005; Westerman et al., 2002). Statistical analyses revealed a trend for an inverse correlation between this learning-memory score and brain Aβ levels, at both 7 months and 13 months of age, which was most robust for Aβ42 levels in the hippocampus (7 months, $r=-0.76$, $P=0.08$; 13 months, $r=-0.77$, $P=0.07$) (at 13 months, $r=-0.64$, for soluble Aβ42, $r=-0.61$, for soluble Aβ40, $r=-0.69$, for total Aβ40, $P>0.1$ in all cases).

Aβ levels in amyloid-forming rats and mice

Tg2576 APP mice have a 5-fold increase of APP compared to non-transgenic mice (Hsiao et al., 1996). As the PSAPP rats had a lower level of APP than that of the Tg2576 mice, but developed amyloid deposits around the same age (~9 months), we compared the level of Aβ by ELISA in age- and region-matched Tg2576 mice and PSAPP rat brain. Levels were also compared to PSAPP mice derived from line Tg2576 that develop plaques much earlier, at ~9 weeks of age. ELISA data for Aβ levels in pre-plaque PSAPP rats (3 months of age), Tg2576 mice (3 months of age), and the pre-plaque PSAPP mice derived from Tg2576 mice (2 months of age) is shown in Table 2. Our results showed that the PSAPP mice had the highest level of Aβ42, and relatively high levels of Aβ40 in both hippocampus and cortex compared to those of the other two transgenic lines. Compared to the Tg2576 mice, the PSAPP rats had a lower level of Aβ42 and Aβ40 in both the hippocampus and cortex; however, among the three transgenic lines, the PSAPP rats had the highest Aβ42:Aβ40 ratio in these two areas, followed by the PSAPP mice, and the Tg2576 mice (Table 2).

Discussion

To our knowledge, the PSAPP transgenic rats described in this study are the first to develop diffuse and compact extracellular amyloid deposits, and to show impairment in LTP and cognitive performance. Although several transgenic rat lines have been described (Echeverria et al., 2004; Folkesson et al., 2007; Ruiz-Opazo et al., 2004), none develop extracellular amyloid deposits or demonstrate cognitive impairment, which was thought to possibly reflect an inability of the rat to form extracellular amyloid. It seems that the reason that other previously published APP transgenic rats (Echeverria et al., 2004; Folkesson et al., 2007; Ruiz-Opazo et al., 2004) failed to develop extracellular amyloid plaques was most likely due to inadequate levels of Aβ that is required for the deposition process to be initiated. We have shown that sufficient elevation of Aβ in a transgenic rat recapitulates the general phenotype of a number of APP and PSAPP transgenic mouse lines including Tg2576 (Hsiao et al., 1996), PDAPP (Games et al., 1995), and PSAPP (Holcomb et al., 1998) transgenic mice (reviewed in McGowan et al., 2006). In general, the rodent models show an age-dependent accumulation of Aβ into diffuse and compact plaques following a spatial distribution pattern similar to that of human AD, and elevation of Aβ correlates with deficits in LTP and/or cognitive impairment. Similar to the transgenic mouse models, the transgenic rat lacks overt neurofibrillary pathology, or cell loss.

Because the PSAPP rats had a lower level of APP protein but developed amyloid deposits around the same time as the Tg2576 mice, we compared the Aβ levels of age-matched PSAPP rats and those of the Tg2576 mice. We also compared Aβ levels between the rats and PSAPP mice that developed Aβ deposits faster — by 9 weeks of age. These comparisons revealed two features. First, the PSAPP mice had the highest level of Aβ42, and relatively high levels of Aβ40 in both hippocampus and cortex compared to those of the other two transgenic lines. Second, compared to the Tg2576 mice, the PSAPP rats had a lower level of Aβ42 and Aβ40 in both the hippocampus and cortex; however, among the three transgenic lines, the PSAPP rats had the highest Aβ42:Aβ40 ratio in these two areas, followed by the PSAPP mice, and the Tg2576 mice. The high Aβ42:Aβ40 ratio found in the PSAPP rats is most likely due to be the combined effects of both a PS1 mutation and the V717F APP mutation — both of which shift Aβ production from Aβ40 to the more amyloidogenic Aβ42 form (Borchelt et al., 1996; Duff et al., 1996; Suzuki et al., 1994). It seems that the rate of Aβ deposition involved two factors: the absolute level of Aβ42, and the Aβ42:Aβ40 ratio. Tg animals that have higher levels of both Aβ42, and Aβ42:Aβ40 ratio (e.g. the PSAPP mice), develop amyloid deposits faster than the animals that are low in these two

Table 1
Levels of soluble and total Aβ 42 and Aβ 40 in the hippocampus and cortex of 7 and 13 month-old PSAPP Tg rats

	7 month-old ($n=3$)		13 month-old ($n=7$)	
	Hippocampus	Cortex	Hippocampus	Cortex
DEA soluble Aβ42	40.79±8.09	11.77±3.69	245.15±71.61	51.70±13.00
Total Aβ42	1020.19±477.79	80.46±28.37	14579.48±2862.24	4570.98±1586.08
DEA soluble Aβ40	34.76±9.01	5.66±2.52	94.86±29.69	23.58±3.69
Total Aβ40	500.44±152.18	92.91±46.88	7924.70±2578.42	456.15±163.02
Aβ42:Aβ40 ratio	1.84±0.37	1.0 7±0.33	3.06±0.68	9.17±1.21

Aβ levels are presented as mean±SEM (pmol/g brain wet tissue). Aβ42:Aβ40 is for total Aβ42 and total Aβ40 levels Total Aβ represents Aβ extracted in formic acid.

Table 2
Comparison of Aβ42 and Aβ40 levels in pre-plaque PSAPP rats, APP mice, and PSAPP mice

Age (months)	Hippocampus			Cortex		
	Aβ40 (pmol/g tissue)	Aβ42 (pmol/g tissue)	Aβ42:Aβ 40	Aβ40 (pmol/g tissue)	Aβ42 (pmol/g tissue)	Aβ42:Aβ40
PSAPP rats (3)	32.18±1.94	15.54±1.43	0.48±0.02	14.25±2.10	9.00±1.19	0.63±0.02
Tg2576APP mice (3)	100.29±1.80	21.02±1.52	0.21±0.01	95.84±2.37	23.21±0.71	0.24±0.00
PSAPP mice (2)	104.64±4.72	30.72±0.56	0.29±0.01	94.46±2.26	34.64±1.27	0.37±0.02

Aβ levels are presented as mean±SEM. $N=3$ for all three groups.

factors (such as the Tg2576 mice). The Aβ42:Aβ40 ratio is also important in determining Aβ deposition in the PSAPP rats: they have much lower overall Aβ levels compared to those of the Tg2576 mice presumably due to lower levels of APP, but they developed amyloid plaques around the same age because they have a higher Aβ42:Aβ40 ratio than that of the Tg2576 mice. An alternative explanation would be the different susceptibility to plaque formation between species.

The PSAPP Tg rats mainly develop diffuse rather than compact amyloid plaques even at a relatively old age (i.e. 19–22 months), despite having a high level of Aβ in the brain. The formation of diffuse verses compact plaques seems to reflect the absolute amount of Aβ42 present as the level of Aβ42 in the forebrain of the Tg rat is less than one-tenth that of the PSAPP mouse which develops extensive compact plaques at a similar age (unpublished data). We also identified compact amyloid plaques in the hippocampus of the Tg rats but not in the cortex, and this correlated with ~three times the level of Aβ42 in the hippocampus compared to cortex, although cortex has a higher Aβ42:Aβ40 ratio. Interestingly, an AAV-mediated gene transfer rat model over-expressing BRI-Aβ42 (Lawlor, 2007) developed only diffuse amyloid plaques. The authors interpreted this as being the result of low cerebral Aβ42 levels in the rat model because BRI-Aβ42 Tg mice overexpressing the same construct have a markedly higher Aβ42 level and develop both diffuse and compact plaques (McGowan, 2005). These studies support the notion that exceeding a certain threshold level of Aβ is required for the deposits to form and that there is a critical level of Aβ42 required for compact plaques to form. In addition, factors other than Aβ itself may also play a role in the transformation of diffuse plaques into compact plaques, such as ApoE4 (Holtzman et al., 2000), interleukin-6 (Hull et al., 1996), and the status of activated microglia cells (Sheng et al., 1997) which may be different in the rat brain.

The PSAPP rats develop very mild amyloid angiopathy (if any), and it is only seen on the leptomeningeal blood vessels, with no detectable amyloid found in the parenchymal blood vessels up to 22 months of age. This may be related to the relatively low level of Aβ40 is only one-third that of similarly aged PSAPP mice that develop vascular amyloid (unpublished data). In general, Aβ40 seems to be the main species involved in cerebral amyloid angiopathy (CAA). Recent studies have shown that Aβ40:Aβ42 ratio is a key factor in determining whether Aβ deposits in blood vessels or in the brain parenchyma. APP transgenic mice expressing the APP E693Q Dutch type mutation had a high Aβ40:Aβ42 ratio and developed extensive CAA with few parenchymal plaques (Herzig et al., 2004), whereas amyloid pathology in these mice was shifted from blood vessels to parenchyma when the Aβ40:Aβ42 ratio was decreased through co-expressing a PS1 FAD mutation (G384A) that favors Aβ42 production. This might be the case in our Tg rats because their Aβ40:Aβ42 ratio is only about 2, whereas the CAA forming Tg2576 and PSAPP mice have an Aβ40:Aβ42 ratio of 5 or 3, respectively (see Table 2). However, other factors in addition to Aβ levels, such as the impaired integrity of the blood brain barrier, increased local Aβ production in the cerebrovascular cells, ageing, arteriosclerosis, and microvascular abnormalities can all contribute to CAA in humans (reviewed in Rensink et al., 2003).

In human AD, synaptic dysfunction can occur at a very early stage in the disease, and memory deficits associated with disease progression are likely to result from pathological changes in the entorhinal cortex and hippocampus — regions critical for the formation of new memories. Synapse density is significantly decreased in the AD brain (Terry et al., 1991). Synapse loss, as reflected by changes in the presynaptic marker synaptophysin, correlates better with cognitive deficits than either plaques or tangles (DeKosky and Scheff, 1990; Dickson et al., 1995; Sze et al., 1997; Terry et al., 1991). Mounting evidence points to alterations in synaptic integrity and plasticity as an early phenotypic manifestation in the pathogenesis of AD, and specifically to Aβ as the underlying factor that induces changes in synaptic function (reviewed in Selkoe, 2002). LTP in the hippocampus is an electrophysiological correlate of synaptic plasticity. Significant deficits in LTP (Jacobsen et al., 2006; Larson et al., 1999; Moechars et al., 1999) and/or basal synaptic transmission (Hsia et al., 1999) in the hippocampus have been demonstrated in several APP overexpressing mouse models of AD, well before the development of Aβ plaques (Selkoe, 2002); thus, the rat model is likely to replicate this important feature of synaptic failure. Indeed, consistent with previous observations in the mouse models, we have demonstrated that deficits in LTP occurred 2–3 months before the appearance of amyloid plaques in the PSAPP rats. Particular forms of Aβ such as low-n oligomeric forms other than Aβ fibrils (e.g. dimers and trimers, Walsh et al., 2002; ADDLs, Klein, 2002, reviewed by Haass and Selkoe, 2007) may underlie the changes in synaptic efficacy, as demonstrated by previous *in vivo* or *in vitro* studies (Lambert et al., 1998; Walsh et al., 2002) (reviewed in Walsh and Selkoe, 2007). Recent findings also suggest that an increase in intracellular Aβ may underlie similar LTP deficits in a transgenic model where parenchymal amyloid deposition occurs after months of high levels of Aβ production (Oddo et al., 2003). Oligomeric Aβ, which can be internalized into neurons from the surrounding milieu, is thought to directly inhibit LTP by interfering with fine mechanisms underlying synaptic plasticity via second messenger systems involved in LTP induction, including the PKA-CREB pathway (Vitolo et al., 2002).

To study the behavioral consequence of increased Aβ and impaired LTP formation, the Morris water maze task was used to

detect impairment in hippocampal-dependent spatial learning and memory (Morris, 1984). As this task is primarily aversively motivated, to exclude the involvement of confounding factors, the open-field test and the elevated plus-maze test were used to detect possible deficits in locomotor function, or differences in emotional status, such as anxiety and fear. No differences were detected between Tg and Wt rats. These findings formed a solid foundation for advanced cognition tests, such as the water maze. No group difference in swim speed was found in the non-spatial learning task, i.e. cued-platform version of water maze test, and Tg rats performed as well as Wt rats. However, for the spatial version of the Morris water maze, the lack of preference in the Tg rats for the target quadrant coupled with the overall poor performance implicated impaired spatial learning and memory. The cognitive deficits were found prior to the appearance of amyloid plaques in young Tg rats, and become more pronounced as the Tg rats age. To investigate the relationship between Aβ levels in the brain and degree of cognitive impairment, correlation analysis was performed between the performance of the Tg rats during the probe trial and levels of soluble and total Aβ in the hippocampus. In both the younger (7 month-old) and older (13 month-old) Tg rats, the correlation analyses revealed a trend for an inverse correlation between the probe trial based learning-memory score and the brain Aβ levels, that was most robust for Aβ42 in the hippocampus. Our results are similar to those observed in transgenic mouse models, for example, performance in the Morris water maze has been reported to be inversely correlated with total hippocampal Aβ42 levels in the APP-PS1(A246E) Tg mouse line (Liu et al., 2003; Puolivali et al., 2002); and an inverse correlation between spatial working memory and amyloid burden was also reported in the PSAPP mice tested in the radial arm water maze (Gordon et al., 2001). However, it should be noted that in the Tg2576 mice, Westerman et al (Westerman et al., 2002) found that the inverse correlation between insoluble Aβ levels and behavioral performance existed only in mice of a certain age, and the correlation disappeared when the data of young and old Tg mice were pooled. They suggested that there must be an age-independent pool of small Aβ assemblies (i.e. Aβ oligomers, such as the Aβ*56, Lesne, 2006) that modified memory function. Together with others, our data further supports a role for Aβ in the impairment of learning and memory, and synaptic plasticity in rodent models. While there is a trend, the data is not robust, and this may reflect that some other species, oligomeric Aβ perhaps, is the real culprit, and measurements of soluble/total Aβ as a surrogate marker are not optimal. This warrants future studies to detail the role of different Aβ forms in cognitive impairment and synaptic dysfunction in the Tg rats at different stages of disease progression.

In conclusion, our data demonstrated that the PSAPP transgenic rat model recapitulated several essential features of AD, including cerebral amyloidosis, synaptic dysfunction, and cognitive deficits that were very similar to the transgenic mouse models. Our data support the view that the development of synaptic dysfunction is independent of amyloid plaque formation, implicating the underlying role of Aβ oligomers or some other toxic species. The current Tg rat model of AD will provide better opportunities for advanced studies, such as serial CSF sampling, electrophysiology (e.g., place cell study), neuroimaging, cell-based transplant manipulations, and complex behavioral testing, and consequently provide more insight into the mechanisms of AD pathogenesis.

Acknowledgments

We thank Dr. Dorothy Flood and Cephalon, Inc. (West Chester, PA) for providing the breeder rats, and Dr. Sonia Jung at Centocor, Inc. (Radnor, PA) for providing the ELISA antibodies for the study. Dr. Peter Davies (Albert Einstein College of Medicine, NY) and Dr. Sam Gandy (Mt. Sinai Medical Center, NY) are thanked for the p-Tau and Ab14 antibodies respectively. We thank Dr. Thomas van Groen (Univ Alabama – Birmingham, AL) for helpful technical suggestions and discussion.

This work was supported by NIH grants NS49442 to OA and NS48447 to KD.

References[1]

Abbott, A., 2004. Laboratory animals: the Renaissance rat. Nature 428, 464–466.

Andorfer, C., et al., 2003. Hyperphosphorylation and aggregation of tau in mice expressing normal human tau isoforms. J. Neurochem. 86, 582–590.

Borchelt, D.R., et al., 1996. Familial Alzheimer's disease-linked presenilin 1 variants elevate Abeta1–42/1–40 ratio in vitro and in vivo. Neuron. 17, 1005–1013.

Chapman, P.F., et al., 1999. Impaired synaptic plasticity and learning in aged amyloid precursor protein transgenic mice. Nat. Neurosci. 2, 271–276.

DeKosky, S.T., Scheff, S.W., 1990. Synapse loss in frontal cortex biopsies in Alzheimer's disease: correlation with cognitive severity. Ann. Neurol. 27, 457–464.

Dickson, D.W., et al., 1995. Correlations of synaptic and pathological markers with cognition of the elderly. Neurobiol. Aging 16, 285–298 discussion 298–304.

Duff, K., et al., 1996. Increased amyloid-beta42(43) in brains of mice expressing mutant presenilin 1. Nature 383, 710–713.

Echeverria, V., et al., 2004. Rat transgenic models with a phenotype of intracellular Abeta accumulation in hippocampus and cortex. J. Alzheimer's Dis. 6, 209–219.

Flood, D.G., et al., 2003. Aβ Deposition in a Transgenic Rat Model of Alzheimer's Disease. Society for Neuroscience, Washington, DC. 2003.

Folkesson, R., et al., 2007. A transgenic rat expressing human APP with the Swedish Alzheimer's disease mutation. Biochem. Biophys. Res. Commun. 358, 777–782.

Games, D., et al., 1995. Alzheimer-type neuropathology in transgenic mice overexpressing V717F beta-amyloid precursor protein. Nature 373, 523–527.

Gordon, M.N., et al., 2001. Correlation between cognitive deficits and Abeta deposits in transgenic APP+PS1 mice. Neurobiol. Aging 22, 377–385.

Gureviciene, I., et al., 2004. Normal induction but accelerated decay of LTP in APP+PS1 transgenic mice. Neurobiol. Dis. 15, 188–195.

Haass, C., Selkoe, D.J., 2007. Soluble protein oligomers in neurodegeneration: lessons from the Alzheimer's amyloid beta-peptide. Nat. Rev., Mol. Cell Biol. 8, 101–112.

Hardy, J., Selkoe, D.J., 2002. The amyloid hypothesis of Alzheimer's disease: progress and problems on the road to therapeutics. Science 297, 353–356.

Herrero, A.I., et al., 2006. Individual differences in anxiety trait are related to spatial learning abilities and hippocampal expression of mineralocorticoid receptors. Neurobiol. Learn. Mem. 86, 150–159.

[1] **Addendum**— A manuscript describing the generation of the present Transgenic rat model by Dr. Flood *et al.* is currently in press at *Neurobiology of Aging* (Flood, D.G., et al., A transgenic rat model of Alzheimer's disease with extracellular Ab deposition, Neurobiology of Aging (2007), doi:10.1016/j.neurobiolaging.2007.10.006).

Herzig, M.C., et al., 2004. Abeta is targeted to the vasculature in a mouse model of hereditary cerebral hemorrhage with amyloidosis. Nat. Neurosci. 7, 954–960.
Holcomb, L., et al., 1998. Accelerated Alzheimer-type phenotype in transgenic mice carrying both mutant amyloid precursor protein and presenilin 1 transgenes. Nat. Med. 4, 97–100.
Holtzman, D.M., et al., 2000. Apolipoprotein E isoform-dependent amyloid deposition and neuritic degeneration in a mouse model of Alzheimer's disease. Proc. Natl. Acad. Sci. U. S. A. 97, 2892–2897.
Hsia, A.Y., et al., 1999. Plaque-independent disruption of neural circuits in Alzheimer's disease mouse models. Proc. Natl. Acad. Sci. U. S. A. 96, 3228–3233.
Hsiao, K., et al., 1996. Correlative memory deficits, Abeta elevation, and amyloid plaques in transgenic mice. Science 274, 99–102.
Hull, M., et al., 1996. Occurrence of interleukin-6 in cortical plaques of Alzheimer's disease patients may precede transformation of diffuse into neuritic plaques. Ann. N.Y. Acad. Sci. 777, 205–212.
Jacobsen, J.S., et al., 2006. Early-onset behavioral and synaptic deficits in a mouse model of Alzheimer's disease. Proc. Natl. Acad. Sci. U. S. A. 103, 5161–5166.
Kauppila, T., et al., 1991. Effects of atipamezole, a novel alpha 2-adrenoceptor antagonist, in open-field, plus-maze, two compartment exploratory, and forced swimming tests in the rat. Eur. J. Pharmacol. 205, 177–182.
Klein, W.L., 2002. Abeta toxicity in Alzheimer's disease: globular oligomers (ADDLs) as new vaccine and drug targets. Neurochem. Int. 41, 345–352.
Kumlin, T., et al., 2007. Mobile phone radiation and the developing brain: behavioral and morphological effects in juvenile rats. Radiat. Res. 168, 471–479.
Kurt, M.A., et al., 2003. Hyperphosphorylated tau and paired helical filament-like structures in the brains of mice carrying mutant amyloid precursor protein and mutant presenilin-1 transgenes. Neurobiol. Dis. 14, 89–97.
Lambert, M.P., et al., 1998. Diffusible, nonfibrillar ligands derived from Abeta1–42 are potent central nervous system neurotoxins. Proc. Natl. Acad. Sci. U. S. A. 95, 6448–6453.
Larson, J., et al., 1999. Alterations in synaptic transmission and long-term potentiation in hippocampal slices from young and aged PDAPP mice. Brain Res. 840, 23–35.
Lawlor, P.A., et al., 2007. Novel rat Alzheimer's disease models based on AAV-mediated gene transfer to selectively increase hippocampal Abeta levels. Mol. Neurodegener. 2, 11.
Lesne, S., et al., 2006. A specific amyloid-beta protein assembly in the brain impairs memory. Nature. 440, 352–357.
Liu, L., et al., 2002. Effects of fimbria–fornix lesion and amyloid pathology on spatial learning and memory in transgenic APP+PS1 mice. Behav. Brain Res. 134, 433–445.
Liu, L., et al., 2003. Abeta levels in serum, CSF and brain, and cognitive deficits in APP+PS1 transgenic mice. Neuroreport 14, 163–166.
McGowan, E., et al., 2005. Abeta42 is essential for parenchymal and vascular amyloid deposition in mice. Neuron. 47, 191–199.
McGowan, E., et al., 2006. A decade of modeling Alzheimer's disease in transgenic mice. Trends Genet. 22, 281–289.
Meerlo, P., et al., 1996. Long-term changes in open field behaviour following a single social defeat in rats can be reversed by sleep deprivation. Physiol. Behav. 60, 115–119.
Moechars, D., et al., 1999. Early phenotypic changes in transgenic mice that overexpress different mutants of amyloid precursor protein in brain. J. Biol. Chem. 274, 6483–6492.
Morris, R., 1984. Developments of a water-maze procedure for studying spatial learning in the rat. J. Neurosci. Methods 11, 47–60.
Oddo, S., et al., 2003. Triple-transgenic model of Alzheimer's disease with plaques and tangles: intracellular Abeta and synaptic dysfunction. Neuron 39, 409–421.
Pellow, S., et al., 1985. Validation of open:closed arm entries in an elevated plus-maze as a measure of anxiety in the rat. J. Neurosci. Methods 14, 149–167.
Planel, E., et al., 2007. Anesthesia leads to tau hyperphosphorylation through inhibition of phosphatase activity by hypothermia. J. Neurosci. 27, 3090–3097.
Puolivali, J., et al., 2002. Hippocampal A beta 42 levels correlate with spatial memory deficit in APP and PS1 double transgenic mice. Neurobiol. Dis. 9, 339–347.
Refolo, L.M., et al., 2001. A cholesterol-lowering drug reduces beta-amyloid pathology in a transgenic mouse model of Alzheimer's disease. Neurobiol. Dis. 8, 890–899.
Rensink, A.A., et al., 2003. Pathogenesis of cerebral amyloid angiopathy. Brain Res. Brain Res. Rev. 43, 207–223.
Ruiz-Opazo, N., et al., 2004. Attenuated hippocampus-dependent learning and memory decline in transgenic TgAPPswe Fischer-344 rats. Mol. Med. 10, 36–44.
Santacruz, K., et al., 2005. Tau suppression in a neurodegenerative mouse model improves memory function. Science 309, 476–481.
Schmidt, S.D., et al., 2005a. Tissue processing prior to protein analysis and amyloid-beta quantitation. Methods Mol. Biol. 299, 267–278.
Schmidt, S.D., et al., 2005b. ELISA method for measurement of amyloid-beta levels. Methods Mol. Biol. 299, 279–297.
Schulz, D., et al., 2007. Behavior on the water maze platform: relationship to learning and open field exploration in aged and adult rats. Brain Res. Bull. 74, 206–215.
Selkoe, D.J., 2001. Alzheimer's disease: genes, proteins, and therapy. Physiol. Rev. 81, 741–766.
Selkoe, D.J., 2002. Alzheimer's disease is a synaptic failure. Science 298, 789–791.
Sheng, J.G., et al., 1997. Neuritic plaque evolution in Alzheimer's disease is accompanied by transition of activated microglia from primed to enlarged to phagocytic forms. Acta Neuropathol. 94, 1–5.
Suzuki, N., et al., 1994. An increased percentage of long amyloid beta protein secreted by familial amyloid beta protein precursor (beta APP717) mutants. Science 264, 1336–1340.
Sze, C.I., et al., 1997. Loss of the presynaptic vesicle protein synaptophysin in hippocampus correlates with cognitive decline in Alzheimer disease. J. Neuropathol. Exp. Neurol. 56, 933–944.
Terry, R.D., et al., 1991. Physical basis of cognitive alterations in Alzheimer's disease: synapse loss is the major correlate of cognitive impairment. Ann. Neurol. 30, 572–580.
Trinchese, F., et al., 2004. Progressive age-related development of Alzheimer-like pathology in APP/PS1 mice. Ann. Neurol. 55, 801–814.
Vitolo, O.V., et al., 2002. Amyloid beta-peptide inhibition of the PKA/CREB pathway and long-term potentiation: reversibility by drugs that enhance cAMP signaling. Proc. Natl. Acad. Sci. U. S. A. 99, 13217–13221.
Walsh, D.M., Selkoe, D.J., 2007. A beta oligomers — a decade of discovery. J. Neurochem. 101, 1172–1184.
Walsh, D.M., et al., 2002. Naturally secreted oligomers of amyloid beta protein potently inhibit hippocampal long-term potentiation in vivo. Nature 416, 535–539.
Wengenack, T.M., et al., 2000. Quantitative histological analysis of amyloid deposition in Alzheimer's double transgenic mouse brain. Neuroscience 101, 939–944.
Westerman, M.A., et al., 2002. The relationship between Abeta and memory in the Tg2576 mouse model of Alzheimer's disease. J. Neurosci. 22, 1858–1867.
Winkler, D.T., et al., 2001. Spontaneous hemorrhagic stroke in a mouse model of cerebral amyloid angiopathy. J. Neurosci. 21, 1619–1627.